Flocculation-flotation harvesting mechanism of Dunaliella salina: From nanoscale interpretation to industrial optimization

Alexandre Besson, Cécile Formosa-Dague, Pascal Guiraud

1   **Flocculation-flotation harvesting mechanism of *Dunaliella salina*: from nanoscale**

2   **interpretation to industrial optimization**

3   Alexandre Besson[1]*, Cécile Formosa-Dague[1,2,3]* and Pascal Guiraud[1,3]

4

5   [1] LISBP, Université de Toulouse, INSA, INRA, CNRS, Toulouse, France

6   [2] LAAS, Université de Toulouse, CNRS, Toulouse, France

7   [3] Fédération de recherche FERMAT, CNRS, Toulouse, France

8

9

10   <u>Corresponding author</u>: Prof. Pascal Guiraud, pguiraud@insa-toulouse.fr

11   *These two authors equally contributed to the work

12

13

14

15 **Abstract**

16 *Dunaliella salina* is a green microalgae species industrially exploited for its capacity to produce

17 important amounts of carotenoid pigments. However in low nitrogen conditions in which they

18 produce these pigments, their concentration is low, which results in harvesting difficulties and high

19 costs. In this work, we propose a new solution to efficiently harvest *D. salina* at the pre-industrial

20 scale, using flocculation/flotation harvesting induced by NaOH addition in the medium. We first

21 show, using numerical simulations and nanoscale atomic force spectroscopy experiments, that

22 sweeping mechanism in formed magnesium hydroxide precipitate is only responsible for *D. salina*

23 flocculation in hypersaline culture medium upon NaOH addition. Based on this understanding of the

24 flocculation mechanism, we then evaluate the influence of several parameters related to NaOH

25 mixing and magnesium hydroxide precipitation and show that NaOH concentration, mixing, and

26 salinity of the medium can be optimized to achieve high flocculation/flotation harvesting efficiencies

27 in laboratory-scale experiments. We finally successfully scale-up the data obtained at lab-scale to a

28 continuous pre-industrial flotation pilot, and achieve up to 80% of cell recovery. This interdisciplinary

29 study thus provides original results, from the nano- to the pre-industrial scale, which allow the

30 successful development of an efficient large-scale *D. salina* harvesting process. We thus anticipate

31 our results to be the starting point for further optimization and industrial use of this

32 flocculation/flotation harvesting technique.

33

34

35

36

37

38

39

40

1. Introduction

Microalgae are receiving increasing attention worldwide as an alternative and renewable source of energy because of their eminent oil producing capacity (Pragya et al., 2013). But the potential of microalgae is in fact even greater and they also represent an important source of biomass and of molecules of interest for the fields of food, feed or health. Indeed, microalgae are unique microorganisms which convert light energy, water and inorganic nutrients into biomass resource rich in value-added products such as lipids, carbohydrates, proteins and pigments (Minhas et al., 2016; Pragya et al., 2013). Among the wide diversity of microalgae (Metting, 1996), *Dunaliella salina,* a halotolerant green microalgae, is among the species currently industrially exploited, as it is one of the most important producer of natural *β*-carotene pigments (Pirwitz et al., 2015; Ambati et al., 2018). Because of this specificity, *D. salina* has been the subject of many studies dedicated to the optimization of its culture conditions (Prieto et al., 2011; Kim et al., 2012; Khadim et al., 2018; Béchet et al., 2018) and of its harvesting (Besson and Guiraud, 2013; Pirwitz et al., 2015; Xiong et al., 2015). Moreover, other studies have showed the utility of this microalgae species in genetic and metabolic engineering (Feng et al., 2014; Anila et al., 2016), and also recently in concrete biomedical applications, for example to reduce tumor growth in mice (Srinivasan et al., 2017).

However, under *β*-carotene production culture conditions (nitrogen deficiency conditions), *D. salina* reaches low cell concentrations which thus has consequences on the energy input and overall cost of their separation from water in industrial processes. In a general manner, several methods can be used for microalgae harvesting, including centrifugation, filtration, flocculation and flotation (Garg et al., 2012). However, most of these methods are synonymous with high costs and energy consumption, often for low efficiency rates. For example, centrifugation, the most commonly used method, consumes a large amount of energy and can cause damages to the cells because of high shear forces (Pragya et al., 2013). Filtration involves using membranes, which, in the case of microalgae separation, can get clogged because of the small size of the cells and/or of the exopolysaccharides they secrete, resulting in high operating costs (Uduman et al., 2010). As for

69   flocculation, it seems to be a promising low-cost approach for large-scale harvesting; however,

70   contamination is a major issue in this technique, as the chemical flocculants classically used to induce

71   flocculation end up in the harvested biomass, and can interfere with the final application of the

72   biomass (food or feed) (Vandamme et al., 2013).

73   In this context, flotation is believed to be a promising harvesting technique that takes

74   advantage of microalgae's natural low density and self-floating tendency (Garg et al., 2012). Assisted

75   flotation consists in air or gas transformed into bubbles rising through a microalgae suspension. As a

76   result, microalgae cells get attached to bubbles and are carried out and accumulated on the surface.

77   Thus flotation allows for low-cost cell harvesting, without necessarily using flocculants that could

78   damage the cells. In addition, it is a relatively rapid operation, which needs low space and has

79   moderate operational costs. However, as both the surface of microalgae and bubbles present a

80   negative charge in aqueous medium (Yang et al., 2001; Garg et al., 2015), and given the low

81   hydrophobicity of microalgae cells, the interactions between cells and bubbles are repulsive, which

82   prevents adhesion, and thus capture and flotation, resulting in the poor efficiency of this harvesting

83   technique.

84   Among the possible strategies to enhance flotation efficiency, natural auto-flocculation is an

85   interesting alternative. There are several known auto-flocculation mechanisms, among which one is

86   based on the precipitation of magnesium ions into magnesium hydroxide at high pH (Sukenik and

87   Shelef, 1984). Such increased pH in the culture medium can result either from the photosynthesis

88   activity of the cells or from the direct addition of OH^-. Then the flocculation of the cells can occur

89   through charge neutralization, *i.e.* through the interaction between the positively charged formed

90   magnesium hydroxide precipitates and cells, through sweeping where cells are entrapped in the

91   massive precipitation of the magnesium hydroxide in the medium, or both (Vandamme et al., 2013).

92   Auto-flocculation of cells at high pH using NaOH addition has already been described for different

93   microalgae species, such as *Chlorella vulgaris* (Wu et al., 2012), or *Phaeodactylum tricornutum* (Wu

94   et al., 2012; Vandamme et al., 2015; Formosa-Dague et al., 2018) and has been showed to occur by

95   both sweeping flocculation and charge neutralization. In the case of *D. salina*, a previous study that

96   we conducted in 2013 showed that addition of NaOH was necessary to increase the pH in the

97   medium, and that further flocculation was caused by sweeping of the cells by forming magnesium

98   hydroxide precipitate (Besson and Guiraud, 2013). In the experimental conditions used in this study,

99   the more NaOH was added, the more magnesium hydroxide was precipitated and the more efficient

100 the flocculation was; a cell recovery up to 100% could be achieved using further flotation. The results

101 obtained also showed that the NaOH flow rate had no influence on the flocculation and further

102 flotation recovery; however they suggested that the type of injection of NaOH, and thus it's mixing in

103 the medium and the speed of magnesium hydroxide precipitation, could have an influence in the

104 final harvesting efficiency.

105   In the work presented here, we will first evidence the only contribution of sweeping

106 mechanism in the flocculation of cells induced by the precipitation of magnesium hydroxide at high

107 pH, and exclude the role of charge neutralization. For that we will first simulate the precipitation of

108 magnesium hydroxide in the medium as a function of the NaOH concentration to understand the

109 behavior of the culture medium during flocculation. Then, we will use recent developments made in

110 the team that consist in using atomic force microscopy (AFM) (Binnig et al., 1986) to probe the

111 interactions between microalgae cells and particles (Formosa-Dague et al., 2018). For that, AFM tips

112 functionalized with magnesium hydroxides particles will be used in force spectroscopy experiments

113 to measure directly, at the piconewton scale, the interactions between these particles and the cells.

114 Then, knowing precisely the flocculation mechanism at play, we will be able to optimize parameters

115 to harvest, in the most effective possible way, *D. salina* cells at laboratory scale but also at pre-

116 industrial scales (suspension flow rate 0.6 m^3/h). For that, we will complete our previous study and

117 determine the role of NaOH mixing in the medium by testing different injection types, agitation and

118 medium salinity, and by evaluating their effects on the flocculation/flotation recovery of the cells at

119 laboratory scale. Based on these results and their interpretation, we will adapt and optimize an

120 injection system to efficiently flocculate and harvest cells by flotation in a pre-industrial continuous

121   cultivation system. This way we will provide a cost-effective solution to efficiently harvest low-

122   concentrated *D. salina* cells at industrial scales, thus contributing to the industrial valorization of this

123   *β*-carotene rich biomass.

124

125   **2. Material and methods**

126   **2.1. Strain and culture conditions**

127   *Dunaliella salina* strain CCAP19/25 (Culture Collection of Algae and Protozoa) was cultivated in

128   dechlorinated tap water containing the following: NaCl (107 g/L); $MgSO_4.7H_2O$ (4.8 g/L); $MgCl_2.6H_2O$

129   (4.0 g/L); $CaCl_2$ (1.1 g/L); KCl (0.1 g/L). A complete nutritive Conway medium (without silicates)

130   (Walne, 1970) was also added. The salinity of this synthetic water is of 10%, the ionic strength of 2.3.

131   This medium was used for all the experiments performed in laboratory. It mimics the medium

132   resulting from the evaporation of see water in which *D. salina* can grow with a limited competition

133   from other microorganisms, used in pre-industrial scale cultures. A *D. salina* strain isolated from

134   saline ponds in Gruissan, Occitanie, France, was also used to evaluate the influence of the strain on

135   the harvesting efficiencies.

136   <u>Laboratory-scale cultures</u>: For AFM experiments, cells were cultivated at 20°C, under agitation (120

137   rpm), in 75 mL non-coated culture flasks (15 mL of culture), 500 mL non-coated culture flasks (150

138   mL of culture). The incubator was equipped with white neon light tubes providing illumination of

139   approximately 40 µmol photons m^{-2} s^{-1} with a photoperiod of 12h light : 12h dark. For flotation

140   experiments, *D. salina* culture was achieved in 10 L glass photobioreactors. The culture was

141   continuously agitated by the gentle bubbling of 0.2 µm filtered atmospheric air (2 L/min).

142   Illumination was provided by daylight fluorescent tubes (OSRAM FQ 965 Biolux) with a photoperiod

143   of 16h light : 8h dark. The temperature of the culture was regulated by air conditioning at 21 ± 3°C.

144   <u>Pre-industrial scale cultures</u>: The pre-industrial experimental site of the Salinalgue research project

145   (2010-2014) was located in a salt marsh on the Mediterranean Sea coast, at Gruissan, Occitanie,

146   France (Latitude: 43.094 N; Longitude: 3.084 E), as fully described in Béchet *et al*. (Béchet et al.,

147 2018). Briefly, cultures were achieved in 4 outdoor raceways of 250 m², containing between 30 and

148 100 m^3. See water concentrated by sun evaporation (salinity of 12%) and disinfected with bleach fed

149 the raceways before being inoculated. The raceways were mixed by paddle wheels and by

150 suspension pumping which was also used to limit the pH to 7.4 by a monitored addition of dissolved

151 CO_2 in the recirculated suspension.

152

153 **2.2. Precipitation model for hydroxide magnesium in the culture medium used**

154 The concentration of magnesium hydroxide, calcium carbonate and dolomite were modeled as a

155 function of the added NaOH concentration in the culture medium. To do so, we simulated the NaOH

156 addition effects and developed a numerical model, using the software Phreeqc, based on the Pitzer

157 equations to simulate the precipitate formation in our culture medium. Indeed, in order to assess the

158 equilibrium state of hypersaline solutions in which *D. salina* is grown and understand the

159 precipitation phenomena involved during NaOH addition, it is necessary to evaluate the activity of

160 species in solution. This requires the evaluation of coefficients of activity, which take into account the

161 various ionic interactions in these complex environments. The models for calculating these activity

162 coefficients are generally based on the coupling of the Debye-Hückel (Debye and Hückel, 1923)

163 theory translating electrostatic ionic interactions, and of the theory of the ionic association that takes

164 into account ionic interactions at short distances. These models are well suited for solutions with

165 ionic strength that does not exceed the one of regular seawater (ionic strength of 0.7). But since the

166 culture of *D. salina* is carried out in a hypersaline environment, the ionic forces encountered in its

167 culture medium exceed the areas of validity of the different ion association models (for a 10% salinity

168 culture medium, the ionic strength is of 2.3). Therefore, the models obtained with these theoretical

169 descriptions of saltwater thermodynamics are not satisfactory for concentrated saline water. In the

170 case of *D. salina*, it was thus necessary to implement other types of models, known as specific ion

171 interaction models, such as the one proposed by Pitzer. The Pitzer model is based on a different

172 thermodynamic approach, and is well suited to evaluate the thermodynamic properties of

173   hypersaline solutions. The model used is based on the Pitzer equations, and allows to simulate the

174   ionic equilibria during the injection of NaOH in our culture medium. The models developed by Pitzer

175   (Pitzer, 1973; Pitzer and Mayorga, 1973, 1974; Pitzer and Kim, 1974; Pitzer, 1975) describes the

176   specific ionic interactions of diverse species in complex media, at high ionic strength. For pure

177   components, this model uses the parameters given by (Pitzer and Mayorga, 1973, 1974). The

178   asymmetric mixing parameters come from Pitzer et and Kim (Pitzer and Kim, 1974; Pitzer, 1975). The

179   whole set of parameters were validated and listed by Harvie *et al.* (Harvie et al., 1984), the relevant

180   database being "pitzer.dat" This database accounts for the significant elements for Mediterranean

181   see water (Na-K-Mg-Ca-H-Cl-S-O-C-Fe-Mn-Ba-Sr-B-Li-Br) with a large spectrum of possible

182   precipitates. Before its application for the simulations presented here, the model has been

183   successfully (Besson, 2013) compared to the experimental results of sea water evaporation proposed

184   by Baseggio (Baseggio, 1974). The composition of the culture medium used for the simulations (Table

185   1) was entered using a temperature of 25°C and a total dissolved carbon concentration of 0.00021

186   mol/kg_water.

187   **Table 1.** Concentrations of the main ions in the culture medium used in simulations in g/L

Na^+	Cl^-	SO_4^{2-}	Mg^{2+}	Ca^{2+}	K^+
42.12	67.08	1.87	0.95	0.39	0.04

188

189   **2.3. Flotation experiments**

190   Due to the small size of the microalgae, Dissolved Air Flotation (DAF) was used to harvest *D. salina*

191   after NaOH-induced flocculation. Figure 1 presents the DAF devices used in this study.

192   Laboratory scale: A detailed presentation of the laboratory scale flotation experiments can be found

193   in Besson & Guiraud (Besson and Guiraud, 2013). DAF experiments were performed in a Multiplace

194   Orchidis™ FTH3 Flottatest. Three flotation-test beakers were run simultaneously, in which 600 mL

195   samples were collected from the algal culture and added to each beaker. Then NaOH was added: in

196   the case of direct NaOH injection, x mL of NaOH at a concentration of 1M was added to the

197   microalgae suspension, as well as 100 - x mL of distilled water. In the case of the diluted NaOH

198   injection, a unique solution containing x mL of NaOH at a concentration of 1M and 100 - x mL of

199   distilled water was added to the microalgae suspension. The volume of NaOH (x) added was

200   calculated depending on the final concentration wanted. This procedure is presented in figure 4a.

201   The depressurization at atmospheric pressure of 200 mL culture medium free of algae and saturated

202   by air at 6 bars for 15 min induced the formation of microbubbles. The recycle ratio (pressurized

203   culture medium volume/initial sample volume) was of 33%. For flocculation, the concentration of the

204   added NaOH solution was calculated taking into account the volume of the culture and the volume of

205   the added white water, so that the pH does not change upon addition of the white waters.

206   <u>Pre-industrial scale</u>: The pre-industrial DAF system was adapted from the CY1 flotation unit proposed

207   by Sérinol (Bram, Occitanie, France), and is presented in Figure 1. Built in 316L stainless steel to avoid

208   corrosion by suspensions at high salinity, this continuous cylindrical (0.6 m of diameter) DAF

209   separation equipment, with a conical bottom, works as an airlift. A cylindrical Clifford delimits the

210   ascending contact zone where the suspension to be treated and the white waters, containing

211   bubbles, mix. At the periphery, the descending annular separation zone is equipped with a vertical

212   lamellar packing to keep the flow as quiet as possible. The nominal descending flow velocity is of 4.0

213   m/h. The flotation tank volume is of 600 L and its maximum flow capacity is of 1 m^3/h. The floated

214   microalgae are mechanically removed from the tank surface by a tunable rotating scrapper. Salted

215   waters identical to the culture medium or recycled from the harvesting are continuously pressurized

216   at 6 bars by a centrifugal pump and saturated with air within a pressurization tank. White waters are

217   produced by passing this pressurized solution through a needle valve. The microbubble size

218   distribution was measured by Laser Diffraction Sizer (Malvern Spraytec): most of the bubbles

219   produced in these saline waters have a diameter smaller than 60 µm (Besson and Guiraud, 2012).

220   NaOH solutions at different concentrations in distilled water were added at different injection places

221   on the supply line at a controlled flow injection using a peristaltic pump. Given that the microalgae

222   suspension flow rate is of 300 L/h, and the final NaOH concentration is of 0.02 mol/L, if a NaOH

223   solution of 0.1 mol/L is injected, the flowrate is of 66 L/h, and if a NaOH solution of 0.2 mol/L is

224   injected, the flowrate is of 0.33 L/h. Flowrates were measured thanks to Khrone Optif lux – 4100

225   electromagnetic flowmeters. For the operating conditions, microalgae suspensions were extracted

226   from the external raceways using a peristaltic pump, into the flotation unit. Simultaneously, the

227   pressurization system was launched and the NaOH solutions were injected on the supply line. The

228   scrapping of the microalgae started as soon as the pressurization system was launched. After one

229   hour at constant operating parameters (three times the time of the continuous state settling),

230   samples required to quantify the separation efficiency (treated suspension) were harvested: the

231   harvesting efficiency was then measured as described below.

232

233   **2.4. Harvesting efficiency quantification**

234   Harvesting efficiency quantification is based on optical density measurements. The harvesting

235   efficiency represents the quantity of algae floated compared to the quantity in the initial suspension:

236   it was evaluated using the following equation:

$$\mathrm{E}(\%) = \left(1 - \frac{\mathrm{OD}a\mathrm{V}a}{\mathrm{OD}i\mathrm{V}i}\right) \times 100$$

237   Where ODi and Vi are the initial optical density at 800 nm and the volume of algal suspension before

238   NaOH addition and flotation, ODa and Va are the optical density at 800 nm of the aqueous phase and

239   the volume of the aqueous phase after injection of pressurized water.

240

241   **2.5. Zeta potential measurements**

242   The global electrical properties of *D. salina* cell surface were assessed by measuring the

243   electrophoretic mobility which corresponds to the velocity of suspended cells exposed to an electric

244   field. To this end, microalgae were harvested by centrifugation (1500 rpm, 3 min), washed two times

245   in sorbitol buffer 375 mM at pH = 10 and resuspended in the same buffer at a final concentration of

246   1.5×10^{6} cell/mL. Using this procedure, electrolytes present in the culture medium do not interfere

247   and only the surface charge of the cells is measured. The electrophoretic mobility was then

248 measured using an automated laser zetameter (Zetasizer NanoZS, Malvern Instruments). Cell

249 suspensions coming from 2 independent cultures were analyzed.

250

251

252

253 **2.6. AFM tip functionalization with hydroxides**

254 To prepare functionalized AFM with $Mg(OH)_2$, MLCT AUWH tips were first dipped into a thin layer of

255 UV-curable glue (NOA63, Norland Edmund Optics), then into a thin layer of $Mg(OH)_2$ particles (Sigma-

256 Aldrich) deposited on a glass slide. Functionalized tips were then put under UV-light for 10 min to

257 allow the glue to cure.

258

259 **2.7. AFM imaging and force spectroscopy experiments**

260 Before AFM experiments, cells were harvested by centrifugation (3000 rpm, 10 min) and washed two

261 times in sorbitol buffer 375 mM at pH = 10. This salt-free buffer is used for force spectroscopy

262 experiments as it allows to accurately measure interactions between the cells and magnesium

263 hydroxide particles functionalized on the AFM tips without introducing a bias from electrolytes

264 present in *D. salina* culture medium. Moreover, the sorbitol present in this buffer keeps the cells

265 from exploding because of the osmotic pressure. Finally, the pH of 10 allows to reproduce the

266 conditions in which the cells are during flocculation induced by addition of NaOH. Cells were then

267 immobilized on polyethylenimine (PEI, Sigma P3143) coated glass slide prepared as previously

268 described (Francius et al., 2008). Briefly, freshly oxygen activated glass slides were covered by a 0.2%

269 PEI solution in deionized water and left for incubation overnight. Then the glass slides were rinsed

270 with deionized water and dried under nitrogen. A total of 1 mL of cell suspension was then deposited

271 on the PEI slides, allowed to stand for 30 min at room temperature, and rinsed with sorbitol buffer

272 375 mM at pH = 10. For force spectroscopy experiments, MLCT AUWH cantilevers with a nominal

273 spring constant of 0.01 N/m, functionalized with hydroxides or not, were used at a constant applied

274   force of 0.25 nN. The cantilevers spring constants were determined using the thermal noise method

275   (Hutter and Bechhoefer, 1993) before each experiment.

276

277

278

279   **3.   Results and discussion**

280   **3.1. Precipitation modeling and AFM force spectroscopy confirm that *D. salina* is flocculated by**

281   **sweeping in magnesium hydroxide precipitate at high pH**

282   In our previous study in 2013 (Besson and Guiraud, 2013), our work evidenced the positive

283   effect of NaOH addition on the flocculation of *D. salina*. Our main results showed indeed an increase

284   in the harvesting efficiency with the addition of NaOH into the medium, up to 80% of cell recovery.

285   While the hypothesis that the flocculation occurred through sweeping in magnesium hydroxide

286   precipitate could be formulated, notably thanks to ions chromatography experiments performed on

287   the suspension before and after flocculation/flotation, no proof of this mechanism were brought.

288   The first part of this study thus focus on providing a full understanding of the NaOH-induced

289   flocculation mechanism. For that we first assessed the equilibrium state of the hypersaline solutions

290   in which *D. salina* is grown to understand the precipitation phenomena involved when flocculating

291   this microalgae using NaOH addition. For that, we used the model described in section 2.2,

292   elaborated from the Pitzer model, to successfully simulate the influence of the addition of NaOH on

293   the ionic equilibria in our culture medium described in Table 1. Results are presented in Figure 2: on

294   this graph, the precipitation of magnesium hydroxide $Mg(OH)_2$ is plotted as a function of the added

295   NaOH concentration. The resulting pH as well as two other precipitate candidate concentrations are

296   also presented. Even if the measure of pH in hypersaline solutions with a high ionic strength presents

297   some problems, the simulated pH profile is similar to experimental measurements, as the one

298   showed in our previous study (Besson and Guiraud, 2013). The pH sharply increases until the

299   beginning of the precipitation of the magnesium hydroxide. Then, it continues to slightly increase

300   until the end of the $Mg(OH)_2$ precipitation, that is to say when all the Mg present in the solution is

301   used. Thus this shows that upon addition of NaOH, magnesium hydroxide precipitation increases

302   until reaching a maximum for a NaOH concentration between 0.08 and 0.1 mol/kg of water, while

303   calcium carbonates precipitation remains non-significant. Thus we can conclude from this simulation

304   that the hypothesis made in our previous study, stating that flocculation of *D. salina* at increased pH,

305   under hypersaline conditions at least, results from the precipitation of only magnesium hydroxide at

306   high pH, among a great number of other possible salts, is correct. While this precipitation creates a

307   gel that entraps the cells and flocculate them through sweeping, the question is now to know if

308   charge neutralization is also involved in this flocculation mechanism, thus to have a full

309   understanding of it.

310   To answer this question we used AFM and performed force spectroscopy experiments using

311   functionalized tips with magnesium hydroxides particles. In this type of experiments, the AFM tip is

312   moved towards the surface until touching it, and then retracted. If an interaction takes place

313   between the tip and the sample, upon retraction, the tip will bend until the force applied is higher

314   than the force of the interaction and the interaction breaks. The tip then goes back to its initial

315   position, which is materialized on AFM retract force curves as a peak, referred to as retract adhesion.

316   The results of these experiments are presented in figure 3, they show in the case of bare AFM tips no

317   adhesion between the tip and the cells, as seen on the retract force curves which present no retract

318   adhesions (Figure 3a and b, n=2400 curves recorded on 6 cells from 2 independent cultures). In the

319   case of tips functionalized by magnesium hydroxides (Figure 3C and d), force curves also show no

320   retract adhesions, thus demonstrating that hydroxide particles do not interact with cells (n=3200

321   curves recorded on 8 cells coming from 2 independent cultures, with 7 different $Mg(OH)_2$ tips). Note

322   that in order to avoid any interaction between electrolytes in the medium and the AFM tips,

323   experiments were performed in a salt-free buffer at pH=10 to make sure only the interactions

324   between the cells and the tips are probed. As no interactions were probed in this buffer, it is then

325   evident that in the hypersaline waters in which *D. salina* grows, these interactions do not occur

326   neither given the high quantity of charged ions that can screen both cells and $Mg(OH)_2$ particles

327   charges. To give an explanation to this absence of interactions between the cells and $Mg(OH)_2$

328   particles, we then performed zeta potential measurements of *D. salina* cells in the same salt-free

329   buffer at high pH (pH = 10), and measured a surface charge of -15.4 ± 0.9 mV (n=8 measurements on

330   cell suspensions coming from 2 independent cultures). Thus the cells do not present a sufficient

331   negative surface charge in our conditions, and do not interact with the positive surface of

332   magnesium hydroxide (Lin and Wang, 2009).

333   Therefore thanks to these simulations and AFM experiments, we are able to confirm the

334   hypothesis we made in our previous study, and show that addition of NaOH in the culture medium

335   precipitates only magnesium hydroxide. This precipitation results in the formation of a gel that is

336   only responsible for entrapping the cells and flocculating them, as AFM experiments proved that

337   charge neutralization is not involved in the case of *D. salina.* Moreover, in further experiments that

338   we performed, $Mg(OH)_2$ already formed was directly added to *D. salina* cultures, which resulted in no

339   flocculation of the cells, thus reinforcing our nanoscale conclusions. This is an interesting point as for

340   all the microalgae species for which pH-induced flocculation has been described, charge

341   neutralization mechanism is always involved (Sukenik and Shelef, 1984; Wu et al., 2012; Vandamme

342   et al., 2012; Nguyen et al., 2014; Vandamme et al., 2015; Formosa-Dague et al., 2018; Branyikova et

343   al., 2018). Indeed, microalgae often have a cell wall, composed of lipids, proteins and

344   polysaccharides. These last ones have a pK_a of 11-12; when the pH increases in the medium, the

345   hydroxyl functions of these polysaccharides are deprotonated, which can give the surface a more

346   important negative charge. As microalgae are usually grown in waters containing calcium or

347   magnesium ions, which precipitate into positively charged particles at high pH, then flocculation

348   occur also thanks to the interaction between these particles and the cells. However in our case, *D.*

349   *salina* cells do not interact with positively charged magnesium hydroxide. Indeed, *Dunaliella* genus is

350   unique in the absence of a rigid polysaccharidic cell wall; cells only present a thin plasma membrane

351   (Oren, 2005; Chen and Jiang, 2009). This thus explains why its surface charge is not more negative at

352 high pH, and thus why charge neutralization is not involved in its flocculation mechanisms in

353 presence of magnesium hydroxide. Thus our results give a full understanding of the mechanism of *D.*

354 *salina* flocculation at high pH; based on these information, we can now evaluate the influence of

355 different parameters, such as NaOH concentration, agitation and salinity in order to determine the

356 best possible separation conditions of the cells from the water, and provide a solution for high-scale

357 harvesting.

358 **3.2. Magnesium hydroxide precipitation phase is determinant for flocculating the cells**

359 Because the flocculation of the cells occur only through sweeping, the precipitation of

360 magnesium hydroxide is then determinant for the successful flocculation/flotation of the cells.

361 Indeed, the precipitation phase must be carried out as homogeneously as possible, so that as much

362 of the sample volume as possible is affected by the trapping of microalgae in the precipitate in

363 formation. Therefore, the conditions for adding NaOH to the suspension should be adapted to

364 optimize its fast mixing. To address this point, we performed flocculation/flotation experiments using

365 two different injection ways (Figure 4a), reaching the same final NaOH concentration. In the first way

366 (direct injection), NaOH (1 mol/L) and water are directly injected in a flotation unit containing the

367 microalgae suspension. In the second way, called here diluted injection, water and NaOH (1 mol/L)

368 are first mixed into one solution, which is further added to the microalgae suspension. Then, in the

369 first case, concentrated NaOH is delivered locally into the medium and in the second case, the local

370 instant concentration of the NaOH solution is reduced. Using these two injection scenarios,

371 flocculation/flotation harvesting was performed: the results, presented in Figure 4b show a clear

372 increase of the harvesting efficiency in the case of diluted injection, for the same final NaOH

373 concentration in the microalgae suspension (black-filled symbols). For example at 0.02 mol/L of final

374 NaOH concentration, the harvesting efficiency using direct injection is of almost 30% whereas using

375 the diluted injection system, it reaches up to 90%. Indeed, in the case of direct injection, a high

376 quantity of concentrated NaOH is locally delivered in the solution, thus the speed of precipitation is

377 increased but only concerns a local area of the suspension. Therefore in this case, only the cells

378   present in this area can be entrapped during the precipitation of magnesium hydroxide. In the case

379   of the diluted injection, the low local concentration allows for a slower precipitation, which then has

380   time to occur in the entire, or at least a larger volume of the microalgae suspension, leading to the

381   entrapment of more cells. This phenomena is further illustrated in Figure 4c; for a final NaOH

382   concentration in the microalgae suspension of 0.02 mol/L, the more diluted the added NaOH solution

383   is, the more efficient the harvesting is. Indeed, for an added NaOH solution of 0.1 mol/L, the

384   flocculation/flotation cell recovery reaches 80% while for NaOH solutions higher than 0.5 mol/L, the

385   harvesting efficiency is reduced to 20%.

386   The results of these experiments then prove that the local concentration of NaOH and the

387   phase of the magnesium hydroxide precipitation is determinant for the harvesting efficiency. While

388   diluted injection allows lowering this local NaOH concentration, to optimize the conditions to reach

389   the best cell separation possible, other parameters such as the agitation and the salinity (quantity of

390   magnesium ions available) of the medium should be taken into account as they will thus also

391   influence the harvesting efficiency.

392

393   **3.3. Agitation and salinity are parameters that influence harvesting efficiency**

394   While diluted injection allows the magnesium hydroxide precipitate to form slowly in the

395   medium, agitation of the medium allows for the precipitation phase to sweep the entire microalgae

396   suspension. In Figure 5a, the effects of different agitation speed on the flocculation/flotation

397   harvesting efficiency were measured. It is clear on this figure that an increase from 20 to 40 rpm

398   allows increasing by approximately a two-fold the cell separation whatever the final NaOH

399   concentration in the microalgae suspension. However, increasing again the agitation speed from 40

400   to 80 rpm do not show the same effect, as the harvesting efficiency in the case of 80 rpm agitation is

401   slightly lower than in the case of 40 rpm. This can be explained by the fact that a too fast agitation

402   can change the structure of the flocs formed and thus have consequences on their capture by the

403   bubbles during flotation. As for the salinity of the medium, to assess its effects on the harvesting

404 efficiency, we performed experiments with *D. salina* cells grown in natural seawaters presenting

405 salinities of 7.5, 12 and 15.2%, using a dilute injection system and an agitation of 40 rpm. The results

406 obtained, presented in Figure 5b, show that the more saline the medium is, the less efficient the

407 harvesting is, whatever the NaOH final concentration. Indeed, while high magnesium concentrations

408 found in highly saline media can be thought, in the case of sweeping flocculation, to enhance

409 harvesting efficiency, it is the opposite effect. In high saline media, the NaOH added directly meets

410 high concentrations of magnesium ions, which induces a fast precipitation of magnesium hydroxide.

411 OH^- has thus no time to reach the entire volume of the suspension. Then a high salinity has similar

412 effects than injection of concentrated NaOH, where only the cells present in the area where fast

413 precipitation of $Mg(OH)_2$ occurs can be entrapped in the precipitate, leading to lower separation

414 rates.

415   Therefore thanks to these experiments, the parameters to reach the best separation rate

416 possible can be optimized: while a dilute injection is needed, the agitation of the medium must be

417 optimized to allow an efficient mixing of NaOH with cells and a $Mg(OH)_2$ precipitation that reaches

418 the entire volume, without having negative effects on the flocs formed. As for the salinity of the

419 culture medium, it needs to be low enough to avoid supersaturation of magnesium hydroxide

420 precipitation, the adequate NaOH concentration depending on the salinity. In order to make sure

421 that only parameters related to the magnesium hydroxide precipitation have an influence on the

422 harvesting efficiency, we also evaluated the influence of the calcium concentration, the *D. salina*

423 strain used, and the nutritive conditions in which the cells are grown. Regarding the influence of the

424 calcium concentration in the medium, Sukenik *et al*. in 1984 have established that the precipitation

425 of calcium and phosphate ions at high pH could induce the flocculation of microalgae cells (Sukenik

426 and Shelef, 1984). The Conway medium used here to cultivate the cells containing phosphate, we

427 thus used waters of different calcium concentrations to evaluate the potential effect of calcium

428 phosphate precipitate on the flocculation of *D. salina*. Our results (Supplementary Data 1) showed no

429 difference in the harvesting efficiencies, thus reinforcing our conclusions on the role of only

430   magnesium hydroxide precipitate in sweeping the cells. The influence of the *D. salina* strain and of its

431   nutritive conditions have then also been evaluated, and showed that for the two strains we tested

432   (the CCAP 19/25 and one other *D. salina* strains isolated from saline ponds in France), the same

433   flocculation/flotation conditions resulted in the same harvesting efficiencies (Supplementary Data 2).

434   Regarding the nutritive conditions in which cells are grown, we chose to focus on nitrogen deficiency

435   conditions. Indeed, the overproduction of *β*-carotene after nitrogen starvation (*i.e.* in conditions of

436   unbalanced growth in response to lack of nitrogen) is a well-documented biological process in *D.*

437   *salina* (Lamers et al., 2012; Bonnefond et al., 2017). We thus chose to address this question as the

438   harvesting method we propose here is intended to be used for industrial use. Our results, with cells

439   grown in nitrogen deficient conditions, showed no difference in the harvesting efficiencies obtained.

440   Thus these two last points show that the flocculation/flotation method that we focus on in this study,

441   when used with the good injection system, agitation and salinity of the medium, is efficient for

442   different *D. salina* strains, in different relevant culture conditions. This demonstrates the robustness

443   of this harvesting method, and thus the parameters identified (NaOH injection, agitation and salinity)

444   can now further be used to develop and adapt a NaOH injection system to efficiently flocculate and

445   harvest cells by flotation in a pre-industrial continuous cultivation/harvesting system.

446

447   **3.4. Development of a pre-industrial harvesting process of *D. salina* by flocculation/flotation.**

448   In this part of the work, the knowledge previously acquired at the laboratory scale is used to

449   harvest *D. salina* cells at high-scales. For that, raceways of 250 m² were built in Gruissan (Occitanie,

450   France) and used to cultivate *D. salina*; an industrial continuous flotation unit (600 L) was adapted

451   and installed on the raceway site to harvest cells using NaOH-induced flocculation/flotation. A

452   network of pumps with controlled flow rates were used to collect the cells from the raceway and

453   bring pressurized water into the flotation unit. For adapting the flotation unit to the specific

454   conditions of *D. salina*, we first faced a technical challenge regarding the size of the bubbles

455   produced in the pilot. Indeed, using a method based on laser light diffraction, we evaluated the size

456 of the bubbles produced by DAF in *D. salina* culture medium (Supplementary Data 3a). These

457 experiments show that in this medium (NaCl concentration of 107 g/L), bubbles have a size of

458 approximately 40 μm, compared to 60-100 μm in freshwater (Edzwald, 1995). Thus the salinity

459 reduces the size of the bubbles, which results in the reduction of their ascending velocity. While this

460 is not a problem at small-scale, because the flotation units consist of one small cylinder (1 L of

461 maximum volume) with only one entry for the pressurized water at the bottom (Figure 1a), at high-

462 scale in a high-dimensioned flotation unit, presenting descending flow zones, it is a problem. For

463 instance, this flotation unit presents holes at the base of the Clifford in order to accentuate the airlift

464 effect and obtain, in nominal functioning conditions, descending speeds of 4 m/h (Figure 1b). We

465 thus roughly calculated the speed of our bubbles, considering them as rigid particles obeying the

466 Stokes law corrected by Oseen (Oseen, 1910; Clift et al., 1978) and found in our conditions an

467 average bubble ascending velocity comprised between 3.6 and 5.4 m/h depending on the

468 contamination degree of their surface (1 and 1.5 mm/s, Supplementary Data 3b). Thus some of the

469 bubbles may not reach the surface and can be aspirated in the flow descending zones of the flotation

470 unit. Thus adaptations directly on the flotation unit were realized, and consisted in decreasing the

471 surface of the holes present at the base of the Clifford to decrease the airlift effect and decrease the

472 velocity in these descending flow zones. This way the rising velocity of the microbubbles is higher

473 than the velocity in the descending flow zones, and thus a functioning similar to what is obtained at

474 the laboratory-scale can be provided.

475 These adaptations made, we then scaled-up the NaOH-induced flocculation/flotation process

476 optimized in batch mode at the laboratory scale, to a continuous pre-industrial scale mode. For that,

477 given the specific flocculation mechanism of *D. salina* by sweeping, it is needed to adapt an injection

478 system that will ensure a good mixing between the cells and the added NaOH, as it is determinant to

479 efficiently flocculate the cells. Given the previous results concerning the salinity of the medium,

480 these experiments were performed in natural seawater at a salinity of 12% that ensured the growth

481 of the cells in the raceway without presenting precipitation supersaturation problems. For the

482   experiments, microalgae cultures were injected into the industrial flotation unit, as well as

483   pressurized waters, through supply lines following the injection system represented in Figure 6a.

484   Note that in this system, the waters used for pressurization are recycled from the flotation unit after

485   microalgae recovery, and may contain also some microalgae. NaOH mixing with microalgae and

486   microbubbles in this system takes place directly in the injection system, and is different depending

487   on its location on this injection system. For instance, in positions 3 and 6 (Figure 6a), mixing will be

488   more efficient than in position 1 and 4 because there the flow rate is the most important and the

489   fluid is already a tri-phase fluid (culture medium, cells and bubbles). Thus to find the best mixing

490   conditions, we chose to inject NaOH at of 0.2 mol/L (final concentration of 0.02 mol/L in the

491   microalgae suspension) at the different places in the injection system represented in red on the

492   schematic representation in Figure 6a. After flocculation/flotation, the harvesting efficiencies were

493   measured: results are presented in Figure 6b. They show that the best cell separation rates, of

494   approximately 60%, are reached when NaOH is injected in the locations 3 and 6, where mixing is the

495   most efficient. If NaOH is injected into the microalgae supply line, the harvesting performance is

496   slightly higher if this injection is made at the outlet of the elbow (position 1), where recirculation

497   phenomena occur because of the 90° bend located just upstream of position 1. However, these

498   performances do not reach those achieved for a NaOH injection in the positions 3 and 6. On the

499   pressurized water supply line, the further away the injection is from the confluence with the

500   suspension feed, the lower the harvesting efficiency is. For instance, the harvesting efficiency is

501   significantly reduced when NaOH is injected in the position 4; this can be explained by the low

502   presence of microalgae in this pipe. The magnesium precipitate needs to be formed in the presence

503   of the cells to best entrap them, thus explaining the lower separation efficiencies reached in the

504   pressurized water supply line.

505   However in these experiments, the maximum harvesting efficiency obtained is of 60%. They

506   were realized with a NaOH solution at a concentration of 0.2 mol/L: as showed before, best

507   separation rates are obtained for diluted NaOH solutions, the best efficiencies being achieved in the

508   case of NaOH solutions of 0.1 mol/L (Figure 4c, 80% of cell separated from water). Thus, in order to

509   optimize the NaOH concentration, using a NaOH injection in the position 3 in the injection system,

510   the experiments were repeated with injected NaOH solutions of different concentrations (final NaOH

511   concentration of 0.02 mol/L). The results are showed in Figure 7, where both the harvesting

512   efficiencies obtained in batch-mode at laboratory scale and in continuous mode at pre-industrial

513   scale are represented. It is clear on this graph that indeed, for a solution of NaOH of 0.1 mol/L, the

514   separation rate reaches 80%, and decreases as the NaOH concentration increases. The interesting

515   point is that for both harvesting modes (batch or continuous), the harvesting efficiencies are the

516   same, thus showing the successful scale-up of our NaOH-induced flocculation/flotation process.

517   Therefore, we could adapt an efficient injection system, allowing to separate in a single pass up to

518   80% of the cells from their culture medium at high scale, and concentrate them by a factor of 230,

519   compared to approximately 20 in laboratory-scale experiments. This difference in the concentration

520   factor is explained by the fact that in the continuous DAF system, the rotation velocity of the

521   scrapper, which removes floated microalgae, and its vertical position in the tank can be tuned in

522   order to adapt the residence time of the foam containing the microalgae at the tank surface. During

523   this residence, the microalgae concentration increases in the foam, due to the liquid drainage by

524   gravity, resulting in higher concentration factors compared to lab-scaled experiments.

525

526   **4. Conclusions**

527   We provide here an interdisciplinary multi-scale study to propose an efficient harvesting

528   method for *D. salina* cells using flocculation/flotation, which can be used at industrial scales.

529   Experiments at the nanoscale as well as simulations allowed first to precisely understand the

530   complete mechanism of flocculation by addition of NaOH in the complex hypersaline medium in

531   which *D. salina* grows. We thus brought strong scientific arguments proving that addition of NaOH in

532   the medium creates a magnesium hydroxide precipitate that entraps the cell and flocculate them

533   through sweeping. Because no other mechanism is involved, the formation of this precipitate, at low

534   speed, in the entire microalgae suspension, is determinant for the harvesting efficiency.

535   Understanding this then led us to evaluate the influence of pertinent parameters to achieve high-

536   efficiency harvesting, all related to the precipitation of $Mg(OH)_2$, that are the NaOH concentration in

537   the medium, the agitation and the salinity of the medium. Our results, in laboratory-scale

538   flocculation/flotation experiments, allowed us to show that the added NaOH solution had to be

539   diluted, the agitation had to be optimal to bring the NaOH in the entire volume without breaking the

540   forming flocs, and that too high salinities were resulting in magnesium hydroxide supersaturation

541   phenomena. It is based on this understanding of the separation mechanisms and on the

542   identification of the influence of different parameters on the harvesting performances that the

543   transition of the process to the pre-industrial scale could be addressed from in an efficient way. For

544   that we focused on the mixing efficiency at the injection site and the NaOH concentration injected to

545   provide optimal parameters and achieve efficient microalgae harvesting at high-scale. Now further

546   studies needs to be done to evaluate with precision the cost and energy consumption of this process

547   at high-scale, and optimize better flocculation conditions to achieve effective harvesting at lower

548   costs. Experiments have already been performed in this way, using slaked lime as a base to induce

549   the precipitation of magnesium hydroxide. Our results so far show promising harvesting efficiencies,

550   achieved at lower cost as calcite is less expensive than NaOH.

551

552

558   **Author contribution**

559   P. G. conceived the project. A. B. and C. F.-D. conceived and performed the experiments. P. G., A. B.

560   and C. F.-D. discussed and interpreted the results. C. F.-D. and A. B. wrote the manuscript. P. G., A. B.,

561   and C. F.-D. reviewed and contributed to the manuscript. All authors approved the final manuscript.

562

563

References

Ambati, R.R., Gogisetty, D., Aswathanarayana, R.G., Ravi, S., Bikkina, P.N., Bo, L., Yuepeng, S., 2018. Industrial potential of carotenoid pigments from microalgae: Current trends and future prospects. Crit. Rev. Food Sci. Nutr. 1–22. https://doi.org/10.1080/10408398.2018.1432561

Anila, N., Simon, D.P., Chandrashekar, A., Ravishankar, G.A., Sarada, R., 2016. Metabolic engineering of Dunaliella salina for production of ketocarotenoids. Photosynth. Res. 127, 321–333. https://doi.org/10.1007/s11120-015-0188-8

Baseggio, G., 1974. The composition of sea water and its concentrates, in: Proceedings of the Fourth Symposium on Salt, 8-12 April 1973. pp. 351–358.

Béchet, Q., Coulombier, N., Vasseur, C., Lasserre, T., Le Dean, L., Bernard, O., 2018. Full-scale validation of an algal productivity model including nitrogen limitation. Algal Res. 31, 377–386. https://doi.org/10.1016/j.algal.2018.02.010

Besson, A., 2013. Etude multi-échelle de la récolte de Dunaliella salina-Développement d'un procédé d'autofloculation-flottation de microalgues (PhD Thesis). Toulouse, INSA.

Besson, A., Guiraud, P., 2013. High-pH-induced flocculation-flotation of the hypersaline microalga Dunaliella salina. Bioresour. Technol. 147, 464–470. https://doi.org/10.1016/j.biortech.2013.08.053

Besson, A., Guiraud, P., 2012. Effects of pH adjustment on Dissolved Air Flotation harvesting of the hypersaline microalga Dunaliella salina., in: 6th International IWA Conference on Flotation for Water and Wastewater Systems. New-York city.

Binnig, G., Quate, C.F., Gerber, C., 1986. Atomic Force Microscope. Phys. Rev. Lett. 56, 930–934.

Bonnefond, H., Moelants, N., Talec, A., Mayzaud, P., Bernard, O., Sciandra, A., 2017. Coupling and uncoupling of triglyceride and beta-carotene production by Dunaliella salina under nitrogen limitation and starvation. Biotechnol. Biofuels 10, 25. https://doi.org/10.1186/s13068-017-0713-4

Branyikova, I., Filipenska, M., Urbanova, K., Ruzicka, M.C., Pivokonsky, M., Branyik, T., 2018. Physicochemical approach to alkaline flocculation of Chlorella vulgaris induced by calcium phosphate

589   precipitates.   Colloids   Surf.   B   Biointerfaces   166,   54–60.

590   https://doi.org/10.1016/j.colsurfb.2018.03.007

591   Chen, H., Jiang, J.-G., 2009. Osmotic responses of Dunaliella to the changes of salinity. J. Cell. Physiol.

592   219, 251–258. https://doi.org/10.1002/jcp.21715

593   Clift, R., Grace, J.R., Weber, M.E., Clift, R., 1978. Bubbles, drops, and particles. Academic press New

594   York.

595   Debye, P., Hückel, E., 1923. The theory of electrolytes. I. Lowering of freezing point and related

596   phenomena. Phys. Z. 24, 185–206.

597   Edzwald, J.K., 1995. Principles and applications of dissolved air flotation. Water Sci. Technol.,

598   Flotation Processes in Water and Sludge Treatment 31, 1–23. https://doi.org/10.1016/0273-

599   1223(95)00200-7

600   Feng, S., Li, X., Xu, Z., Qi, J., 2014. Dunaliella salina as a novel host for the production of recombinant

601   proteins. Appl. Microbiol. Biotechnol. 98, 4293–4300. https://doi.org/10.1007/s00253-014-5636-4

602   Formosa-Dague, C., Gernigon, V., Castelain, M., Daboussi, F., Guiraud, P., 2018. Towards a better

603   understanding of the flocculation/flotation mechanism of the marine microalgae Phaeodactylum

604   tricornutum under increased pH using atomic force microscopy. Algal Res. 33, 369–378.

605   https://doi.org/10.1016/j.algal.2018.06.010

606   Francius, G., Tesson, B., Dague, E., Martin-Jézéquel, V., Dufrêne, Y.F., 2008. Nanostructure and

607   nanomechanics of live Phaeodactylum tricornutum morphotypes. Environ. Microbiol. 10, 1344–1356.

608   https://doi.org/10.1111/j.1462-2920.2007.01551.x

609   Garg, S., Li, Y., Wang, L., Schenk, P.M., 2012. Flotation of marine microalgae: effect of algal

610   hydrophobicity. Bioresour. Technol. 121, 471–474. https://doi.org/10.1016/j.biortech.2012.06.111

611   Garg, S., Wang, L., Schenk, P.M., 2015. Flotation separation of marine microalgae from aqueous

612   medium. Sep. Purif. Technol. 156, 636–641. https://doi.org/10.1016/j.seppur.2015.10.059

613 Harvie, C.E., Møller, N., Weare, J.H., 1984. The prediction of mineral solubilities in natural waters:

614 The Na-K-Mg-Ca-H-Cl-SO4-OH-HCO3-CO3-CO2-H2O system to high ionic strengths at 25°C. Geochim.

615 Cosmochim. Acta 48, 723–751. https://doi.org/10.1016/0016-7037(84)90098-X

616 Hutter, J.L., Bechhoefer, J., 1993. Calibration of atomic-force microscope tips. Rev. Sci. Instrum. 64,

617 1868–1873.

618 Khadim, S.R., Singh, P., Singh, A.K., Tiwari, A., Mohanta, A., Asthana, R.K., 2018. Mass cultivation of

619 Dunaliella salina in a flat plate photobioreactor and its effective harvesting. Bioresour. Technol. 270,

620 20–29. https://doi.org/10.1016/j.biortech.2018.08.071

621 Kim, W., Park, J.M., Gim, G.H., Jeong, S.-H., Kang, C.M., Kim, D.-J., Kim, S.W., 2012. Optimization of

622 culture conditions and comparison of biomass productivity of three green algae. Bioprocess Biosyst.

623 Eng. 35, 19–27. https://doi.org/10.1007/s00449-011-0612-1

624 Lamers, P.P., Janssen, M., De Vos, R.C.H., Bino, R.J., Wijffels, R.H., 2012. Carotenoid and fatty acid

625 metabolism in nitrogen-starved Dunaliella salina, a unicellular green microalga. J. Biotechnol. 162,

626 21–27. https://doi.org/10.1016/j.jbiotec.2012.04.018

627 Lin, J.X., Wang, L., 2009. Adsorption of dyes using magnesium hydroxide-modified diatomite.

628 Desalination Water Treat. 8, 263–271. https://doi.org/10.5004/dwt.2009.786

629 Metting, F.B., 1996. Biodiversity and application of microalgae. J. Ind. Microbiol. 17, 477–489.

630 https://doi.org/10.1007/BF01574779

631 Minhas, A.K., Hodgson, P., Barrow, C.J., Adholeya, A., 2016. A Review on the Assessment of Stress

632 Conditions for Simultaneous Production of Microalgal Lipids and Carotenoids. Front. Microbiol. 7.

633 https://doi.org/10.3389/fmicb.2016.00546

634 Nguyen, T.D.P., Frappart, M., Jaouen, P., Pruvost, J., Bourseau, P., 2014. Harvesting Chlorella vulgaris

635 by natural increase in pH: effect of medium composition. Environ. Technol. 35, 1378–1388.

636 https://doi.org/10.1080/09593330.2013.868531

637 Oren, A., 2005. A hundred years of Dunaliella research: 1905–2005. Saline Syst. 1, 2.

638 https://doi.org/10.1186/1746-1448-1-2

639 Oseen, C.W., 1910. Stokes' Formula and a Related Theorem in Hydrodynamics. Ark. Mat Astron Fys.
640 6, 20.

641 Pirwitz, K., Rihko-Struckmann, L., Sundmacher, K., 2015. Comparison of flocculation methods for
642 harvesting Dunaliella. Bioresour. Technol. 196, 145–152.
643 https://doi.org/10.1016/j.biortech.2015.07.032

644 Pitzer, K.S., 1975. Thermodynamics of electrolytes. V. Effects of higher-order electrostatic terms. J.
645 Solut. Chem. 4, 249–265.

646 Pitzer, K.S., 1973. Thermodynamics of electrolytes. I. Theoretical basis and general equations. J. Phys.
647 Chem. 77, 268–277. https://doi.org/10.1021/j100621a026

648 Pitzer, K.S., Kim, J.J., 1974. Thermodynamics of electrolytes. IV. Activity and osmotic coefficients for
649 mixed electrolytes. J. Am. Chem. Soc. 96, 5701–5707.

650 Pitzer, K.S., Mayorga, G., 1974. Thermodynamics of electrolytes. III. Activity and osmotic coefficients
651 for 2–2 electrolytes. J. Solut. Chem. 3, 539–546.

652 Pitzer, K.S., Mayorga, G., 1973. Thermodynamics of electrolytes. II. Activity and osmotic coefficients
653 for strong electrolytes with one or both ions univalent. J. Phys. Chem. 77, 2300–2308.

654 Pragya, N., Pandey, K.K., Sahoo, P.K., 2013. A review on harvesting, oil extraction and biofuels
655 production technologies from microalgae. Renew. Sustain. Energy Rev. 24, 159–171.
656 https://doi.org/10.1016/j.rser.2013.03.034

657 Prieto, A., Pedro Cañavate, J., García-González, M., 2011. Assessment of carotenoid production by
658 Dunaliella salina in different culture systems and operation regimes. J. Biotechnol. 151, 180–185.
659 https://doi.org/10.1016/j.jbiotec.2010.11.011

660 Srinivasan, R., Chaitanyakumar, A., Mageswari, A., Gomathi, A., Pavan Kumar, J.G.S., Jayasindu, M.,
661 Bharath, G., Shravan, J.S., Gothandam, K.M., 2017. Oral administration of lyophilized Dunaliella
662 salina, a carotenoid-rich marine alga, reduces tumor progression in mammary cancer induced rats.
663 Food Funct. 8, 4517–4527. https://doi.org/10.1039/c7fo01328k

664   Sukenik, A., Shelef, G., 1984. Algal autoflocculation--verification and proposed mechanism.

665   Biotechnol. Bioeng. 26, 142–147. https://doi.org/10.1002/bit.260260206

666   Uduman, N., Qi, Y., Danquah, M.K., Forde, G.M., Hoadley, A., 2010. Dewatering of microalgal

667   cultures: A major bottleneck to algae-based fuels. J. Renew. Sustain. Energy 2, 012701.

668   https://doi.org/10.1063/1.3294480

669   Vandamme, D., Foubert, I., Fraeye, I., Meesschaert, B., Muylaert, K., 2012. Flocculation of Chlorella

670   vulgaris induced by high pH: Role of magnesium and calcium and practical implications. Bioresour.

671   Technol. 105, 114–119. https://doi.org/10.1016/j.biortech.2011.11.105

672   Vandamme, D., Foubert, I., Muylaert, K., 2013. Flocculation as a low-cost method for harvesting

673   microalgae   for   bulk   biomass   production.   Trends   Biotechnol.   31,   233–239.

674   https://doi.org/10.1016/j.tibtech.2012.12.005

675   Vandamme, D., Pohl, P.I., Beuckels, A., Foubert, I., Brady, P.V., Hewson, J.C., Muylaert, K., 2015.

676   Alkaline flocculation of Phaeodactylum tricornutum induced by brucite and calcite. Bioresour.

677   Technol. 196, 656–661. https://doi.org/10.1016/j.biortech.2015.08.042

678   Walne, P.R., 1970. Studies on the food value of nineteen genera of algae to juvenile bivavlves of the

679   genera Ostrea, Crassostrea, Mercenaria and Mytillus. Fish. Invest Lond 5, 62.

680   Wu, Z., Zhu, Y., Huang, W., Zhang, C., Li, T., Zhang, Y., Li, A., 2012. Evaluation of flocculation induced

681   by pH increase for harvesting microalgae and reuse of flocculated medium. Bioresour. Technol. 110,

682   496–502. https://doi.org/10.1016/j.biortech.2012.01.101

683   Xiong, Q., Pang, Q., Pan, X., Chika, A.O., Wang, L., Shi, J., Jia, L., Chen, C., Gao, Y., 2015. Facile sand

684   enhanced electro-flocculation for cost-efficient harvesting of Dunaliella salina. Bioresour. Technol.

685   187, 326–330. https://doi.org/10.1016/j.biortech.2015.03.135

686   Yang, C., Dabros, T., Li, D., Czarnecki, J., Masliyah, J.H., 2001. Measurement of the Zeta Potential of

687   Gas Bubbles in Aqueous Solutions by Microelectrophoresis Method. J. Colloid Interface Sci. 243, 128–

688   135. https://doi.org/10.1006/jcis.2001.7842

689

Figure captions

Figure 1. Schematic representation of the dissolved air flotation devices used. (a) DAF device used

at the laboratory-scale and (b) at the pre-industrial scale (with the courtesy of Serinol). In (b), the

position of the NaOH line and needle valve depend on the injection site chosen to perform the

experiment.

Figure 2. Simulating the influence of the addition of NaOH on the ionic equilibria in *D. salina*

culture medium. Phreeqc simulation of the pH and precipitates formation upon addition of NaOH in

the culture medium.

Figure 3. Probing the interactions between *D. salina* cells and magnesium hydroxides. (a) Histogram

representing the adhesion force distribution recorded on cells in sorbitol buffer at pH = 10 with bare

AFM tips, and (b) histogram representing the rupture distance distributions in these conditions. The

inset in (a) is an optical image of a *D. salina* cell and of the AFM probe; the inset in (b) shows

representative retract force curves obtained. (c) Histogram representing the adhesion force

distribution recorded on cells in sorbitol buffer at pH = 10 with $Mg(OH)_2$ functionalized AFM tips, and

(d) histogram representing the rupture distance distributions in these conditions. Inset in (d) shows

representative retract force curves obtained.

Figure 4. Influence of the NaOH injection way on the harvesting efficiencies. (a) Scheme

representing the principle of the two injection systems used. In each case, the same quantity of

NaOH is added, and the same final NaOH concentration in the microalgae suspension is reached. (b)

Flocculation/flotation harvesting efficiencies obtained for a final NaOH concentration of 0.02 mol/L

using the direct injection system (open symbols) or the diluted injection system (black-filled symbols)

and in both case a NaOH solution of 1 mol/L. (c) Flocculation/flotation harvesting efficiencies

715   obtained for a final NaOH concentration of 0.02 mol/L using the diluted injection system and injected

716   NaOH solutions of different concentrations.

717   **Figure 5. Influence of agitation and salinity on the harvesting efficiencies.** (a) Influence of the

718   agitation speed on the harvesting efficiency obtained for a final NaOH concentration of 0.02 mol/L

719   using the diluted injection system with a NaOH solution of 1 mol/L. Open diamonds symbols

720   correspond to an agitation speed of 20 rpm, black-filled circles correspond to 40 rpm, and black-filled

721   diamonds correspond to 80 rpm.   (b) Influence of the salinity of the culture medium on the

722   harvesting efficiency obtained for a final NaOH concentration of 0.02 mol/L using the diluted

723   injection system with a NaOH solution of 1 mol/L. Cross symbols correspond to a salinity of 7.5%,

724   open-squares correspond to a salinity of 12% and open-circles correspond to a salinity of 15.2%.

725

726   **Figure 6. Adaptation of the NaOH injection system for high-scale harvesting.** (a) Schematic and

727   simplified representation of the injection system of the microalgae suspension and of the pressurized

728   water into the industrial flotation unit. Red crosses represents the positions on the injection system

729   where NaOH can be injected. The waters sued for pressurization are recycled from the flotation unit

730   after cell recovery and may contain some microalgae. (b) Influence of the NaOH injection position on

731   the flocculation/flotation harvesting efficiency obtained for a final NaOH concentration of 0.02 mol/L

732   and a NaOH solution of 0.2 mol/L.

733

734   **Figure 7. Influence of the injected NaOH concentration on the harvesting efficiency.**

735   Flocculation/flotation harvesting efficiencies obtained for a final NaOH concentration of 0.02 mol/L

736   injected NaOH solutions of different concentrations. Results obtained in batch mode using diluted

737   injection (open diamond symbols) or in continuous mode with NaOH injection in position 3

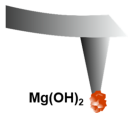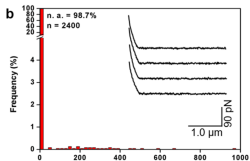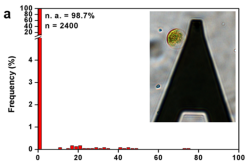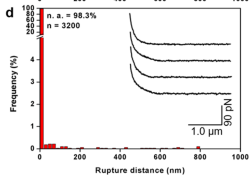738   represented in Figure 5a (black-filled diamond symbols).

739

740

a

Cells + NaOH

Floated microalgae

Pressurization tank

Flotation beakers

Treated suspension exit

White waters entry

b

Scraper

Microalgae entry

Floated microalgae

Floated microalgae exit

Clifford

Lamellar Pack

Treated suspension exit

NaOH entry

Needle valve

White waters

Pressurization system

Air entry

a

Direct injection

x mL of NaOH

(100-x) mL of water

Diluted injection

Homogenization

x mL of NaOH

(100-x) mL of water

b Harvesting efficiency vs Final NaOH concentration (mol/L)

c Harvesting efficiency vs Concentration of added NaOH solution (mol/L)

a

D. salina raceway

Microalgae

Floated microalgae

Seawater pressurization tank

Pressurized water

Flotation unit

Recycled water

b

Figure b: Harvesting efficiency by injection place — bar chart showing values 56.0% (1), 46.3% (2), 63.4% (3), 24.4% (4), 54.9% (5), 60.7% (6). X-axis: Injection place. Y-axis: Harvesting efficiency (0%–100%).

Table 1. Concentrations of the main ions in the culture medium used in g/L

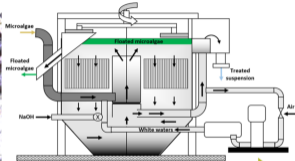| Na^+	Cl^-	SO_4^{2-}	Mg^{2+}	Ca^{2+}	K^+
42.12	67.08	1.87	0.95	0.39	0.04

AFM to probe *D. salina* interactions with Mg(OH)₂ particles

20 µm
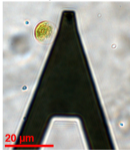
Sweeping of cells and microbubbles during Mg(OH)₂ precipitation

Cells

Bubbles

100 µm
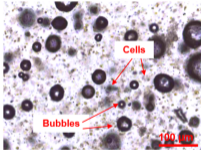
Industrial harvesting of *D. salina* by flocculation/flotation

Microalgae

Floated microalgae

Floated/microalgae

NaOH

White waters

Treated suspension

Air

Molecular scale

Pre-industrial scale